



Immunostimulatory efficacy and protective potential of putative TgERK7 protein in mice experimentally infected by *Toxoplasma gondii*

Zhong-Yuan Li^{a,b,c}, Hai-Ting Guo^a, Guillermo Calderón-Mantilla^d, Jun-Jun He^b, Jin-Lei Wang^b, Boyan B. Bonev^e, Xing-Quan Zhu^{b,*}, Hany M. Elsheikha^{f,**}

^a Guangxi Key Laboratory of Brain and Cognitive Neuroscience, College of Basic Medicine, Guilin Medical University, Guilin, Guangxi, 541199, China

^b State Key Laboratory of Veterinary Etiological Biology, Key Laboratory of Veterinary Parasitology of Gansu Province, Lanzhou Veterinary Research Institute, Chinese Academy of Agricultural Sciences, Lanzhou, Gansu, 730046, China

^c College of Animal Science and Technology, Anhui Agricultural University, Hefei, Anhui, 230036, China

^d Universidad de La Sabana, Campus del Puente del Común, Km. 7, Autopista Norte de Bogotá. Chía, Cundinamarca, Colombia

^e School of Life Sciences, University of Nottingham, Queen's Medical Centre, Nottingham NG7 2UH, UK

^f Faculty of Medicine and Health Sciences, School of Veterinary Medicine and Science, University of Nottingham, Sutton Bonington Campus, Loughborough, LE12 5RD, UK

ARTICLE INFO

Keywords:

Toxoplasma gondii

TgERK7

Immunostimulatory efficacy

Protective potential

Infection

ABSTRACT

The extracellular signal-regulated kinases (ERKs) serve as important determinants of cellular signal transduction pathways, and hence may play important roles during infections. Previous work suggested that putative ERK7 of *Toxoplasma gondii* is required for efficient intracellular replication of the parasite. However, the antigenic and immunostimulatory properties of TgERK7 protein remain unknown. The objective of this study was to produce a recombinant TgERK7 protein *in vitro* and to evaluate its effect on the induction of humoral and T cell-mediated immune responses against *T. gondii* infection in BALB/c mice. Immunization using TgERK7 mixed with Freund's adjuvants significantly increased the ratio of CD3e⁺CD4⁺T/CD3e⁺CD8a⁺T lymphocytes in spleen and elevated serum cytokines (IFN- γ , IL-2, IL-4, IL-10, IL-12p70, IL-23, MCP-1, and TNF- α) in immunized mice compared to control mice. On the contrary, immunization did not induce high levels of serum IgG antibodies. Five predicted peptides of TgERK7 were synthesized and conjugated with KLH and used to analyze the antibody specificity in the sera of immunized mice. We detected a progressive increase in the antibody level only against TgERK7 peptide A (DEVDKHVLKRYD). Antibody raised against this peptide significantly decreased intracellular proliferation of *T. gondii* *in vitro*, suggesting that peptide A can potentially induce a protective antibody response. We also showed that immunization improved the survival rate of mice challenged with a virulent strain and significantly reduced the parasite cyst burden within the brains of chronically infected mice. Our data show that TgERK7-based immunization induced TgERK7 peptide A-specific immune responses that can impart protective immunity against *T. gondii* infection. The therapeutic potential of targeting ERK7 signaling pathway for future toxoplasmosis treatment is warranted.

1. Introduction

The apicomplexan protozoan parasite *Toxoplasma gondii* is an opportunistic protozoan that can infect all warm-blooded animals and approximately one-third of the world's human population (Chen et al., 2017; Kim and Weiss, 2008; Sasai et al., 2018; Schlüter et al., 2014). *T. gondii* infection can result in serious illness particularly in infants infected *in utero* and in immunocompromised patients (Elsheikha, 2008). This parasite secretes proteins (e.g. cyclophilin-18, TgMIF and heat-

shock cognate protein 70 T) to manipulate host cell machinery in order to sustain its own growth and survival within the host (Dvorakova-Hortova et al., 2014; Ibrahim et al., 2010; Kortagere, 2012; Sommerville et al., 2013; Szabo and Finney, 2017). Other strategies employed by *T. gondii* to establish an infection include secretion of effectors that interfere with host's signaling pathways (Hakimi et al., 2017), manipulation of the migratory ability of infected host cells (Kanatani et al., 2017), inhibition of apoptosis of host cells (Chavarría-Smith and Vance, 2015), avoiding autophagy (Portillo et al., 2017), and

* Corresponding authors at: Lanzhou Veterinary Research Institute, Chinese Academy of Agricultural Sciences, 1 Xujiaping, Yanchang Road, Lanzhou, Gansu, 730046, China.

** Corresponding authors at: School of Veterinary Medicine and Science, University of Nottingham, Sutton Bonington Campus, Loughborough, LE12 5RD, UK.

E-mail addresses: zhuxingquan@caas.cn (X.-Q. Zhu), hany.elsheikha@nottingham.ac.uk (H.M. Elsheikha).

altering host cell cycle (Francia and Striepen, 2014; Lüder and Rahman, 2017). This intricate level of interaction between *T. gondii* and host cells highlights the importance of understanding the pathogenesis of *T. gondii* infection.

The mitogen-activated protein kinase (MAPK)/ERK pathway plays roles in the proliferation, differentiation, and apoptosis of mammalian cells (Cargnello and Roux, 2011; Kyosseva, 2004). Several MAPK/ERK proteins have been identified in protozoa, such as *Giardia lamblia* (Ellis et al., 2003), *Leishmania mexicana* (Bengs et al., 2005), *Plasmodium falciparum* (Lye et al., 2006), and *T. gondii* (Brumlik et al., 2004; Huang et al., 2011), indicating the presence of this mammalian-like MAPK/ERK signaling pathway in various parasites. Also, two MAPK/ERK proteins have been identified in *T. gondii*: TgMAPK1, a stress-response MAPK, which is an important virulence determinant that affects *T. gondii* stage differentiation and proliferation (Brumlik et al., 2004, 2013) and putative TgERK7 protein (also known as TgMAPK2), which is associated with intracellular proliferation of *T. gondii*, where *erk7* gene-knockout strain exhibited extended asexual cycles within host cells (Li et al., 2016). These findings suggest that TgERK7 protein is a critical determinant of *T. gondii* pathogenesis and may play a role in stimulation of host immune responses during *T. gondii* infection, and can therefore be a candidate vaccine antigen.

In this study, a recombinant TgERK7 protein-based vaccine was tested in BALB/c mice in order to examine the potential of TgERK7 to induce effective immunity that protects against *T. gondii* infection. We also investigated several immune response parameters, such as antibody (Ab) titers, cytokine levels, T-cell populations in order to evaluate the extent of the immune response that this vaccine can elicit. The immunogenicity of five predicted peptides of TgERK7 and the full length TgERK7 was examined using sera from immunized mice. Furthermore, the growth inhibitory activity of antibodies raised against the five TgERK7 peptides against *T. gondii* was studied *in vitro*.

2. Materials and methods

2.1. Cell lines, parasites and animals

African green monkey kidney (Vero) cells were used as feeder cells to maintain *T. gondii* GT1 strain (Genotype I). Human foreskin fibroblast (HFF) cells were used to evaluate parasite replication *in vitro*. Culture conditions, including cell passaging, were performed as previously described (Braun et al., 2013; Li et al., 2016). Density gradient centrifugation using Percoll (GE Healthcare, Uppsala, Sweden) was used to isolate the tachyzoites as previously described (Omata et al., 1999). The cysts of *T. gondii* PRU strain (Genotype II) were isolated from brain homogenates of chronically infected Kunming mice. Purified tachyzoites and brain cysts of *T. gondii* were counted microscopically using a hemocytometer and used in the subsequent experiments.

Six- to 8-week-old female BALB/c mice were purchased from the Laboratory Animal Center of Lanzhou University (Lanzhou, China). Mouse food and bedding materials were provided by Beijing Keao corporation (<http://u6452366.b2bname.com>). Mice were housed in cages under specific-pathogen-free (SPF) conditions in high-density Touch Screen Mouse IVC (FENGSHI, Suzhou, China) without any treatment for a week, in order to allow time for acclimatization and reduce stress before immunization. The experimental protocols were approved by the Animal Ethics and Administration Committee of Lanzhou Veterinary Research Institute, Chinese Academy of Agricultural Sciences (Approval No. LVRIAEC2012–011). All experiments were conducted in accordance with the guidelines of the Animal Ethics Procedures of the People's Republic of China. Every effort was made to avoid any unnecessary discomfort and pain to the animals.

2.2. Construction of pET-erk7 plasmid and protein expression

The coding sequence of *T. gondii erk7* gene was amplified by PCR

using two specific primers (forward primer: 5'-GGAATTCATATGAAACACCATCATCATCATCAGATGAGTGACGAGGTCGACAAAC-3' and reverse primer: 5'-CCGGAATTCCTATCAGCTGTTGTATGTCTTGAC-3'). This primer set was designed according to the sequence of the reference *T. gondii* GT1 strain (ToxoDB: TGGT1_233010) and included *NdeI* and *EcoRI* restriction sites (underlined) and the his-tag (double underlined). Total RNA of GT1 tachyzoites was extracted using the E.Z.N.A.® Total RNA Kit I (Omega, Georgia, USA).

The amplification reaction was performed according to the instructions of the PrimeScript™ One Step RT-PCR Kit Ver2 (TaKaRa, Dalian, China) as follows: reverse transcription at 50 °C for 0.5 h; RTase inactivation at 95 °C for 2 min; followed by 35 cycles with initial denaturation at 95 °C for 1 min, annealing at 56 °C for 0.5 min, and extension at 72 °C for 2 min; and a final extension at 72 °C for 10 min. The amplified product was isolated using the E.Z.N.A.® Gel Extraction Kit (Omega) and ligated into the pMD18-T simple linear vector (TaKaRa) to construct the pMD-erk7 plasmid. A plasmid with *erk7* sequence was cut with the restriction enzymes *NdeI* and *EcoRI* (NEB, Beijing, China) and ligated into the pET-30a prokaryotic expression vector that was restricted with the same restriction enzymes (Novagen, Wisconsin, USA). The sequence of the resulting recombinant pET-erk7 plasmid was confirmed by DNA sequencing. The recombinant pET-erk7 plasmid containing the TgERK7 was transformed into chemically competent *Escherichia coli* BL21(DE3) cells, where protein expression was performed by inducing the *lac* promoter for expression of T7 RNA polymerase with isopropyl-β-D-thiogalactoside (IPTG, Promega, Wisconsin, USA). The expressed TgERK7 protein with N-terminal 6 × His tags was purified using chromatography column packed with 5 mL of Ni-NTA His-Bind® Resin (Novagen), according to the manufacturer's instruction.

2.3. Generation of peptide-specific antibodies

The amino acid sequence of the putative TgERK7 protein was deduced from *T. gondii erk7* gene (ToxoDB: TGGT1_233010) using the DNASTAR software (<http://www.dnastar.com/>), and five antigenic epitopes were selected based on the flexible region, surface probability, hydrophilicity and antigenic index analyses (Antunes et al., 2015; Berzofsky, 1985); these are shown in Table 1. The synthesis, purification and conjugation with Keyhole Limpet Hemocyanin (KLH) of the five peptides were performed by the SBS Genetech Co., Ltd. (Beijing, China). The production of rabbit polyclonal antibodies against these five peptides, was performed according to the standard 70-day rabbit immunization protocol provided by Thermo Fisher Scientific Inc. (<https://www.thermofisher.com>). All antibodies (Table 1) were purified using BeaverBeads™ Protein A/G Matrix Antibody Purification Kit (BeaverBio, Suzhou, China).

2.4. SDS-PAGE and Western blot analysis

The expressed protein in the lysates obtained from bacterial cells transfected with the recombinant pET-erk7 plasmid or the empty pET-30a plasmid, was analyzed via sodium dodecyl sulfate-polyacrylamide gel electrophoresis (SDS-PAGE), and Western blotting as previously described (Nabi et al., 2017). For Western blot analysis, the separated protein was electrophoretically transferred to a polyvinylidene fluoride

Table 1
The details of TgERK7 peptides and the corresponding antibodies.

Peptide	Sequence (N' - C')	Location	Corresponding antibody
A	DEVDKHVLRYKD	3–14	αA
B	TGRSPEDVDAVK	237–249	αB
C	IKKKHDQRRHRTA	346–358	αC
D	GSFVRDRPPAYA	461–472	αD
E	HGPVRAKTDTHT	647–658	αE

(PVDF) membrane. The membranes were incubated with a 1:1,000 dilution of rabbit anti-*T. gondii* TgERK7 peptide A-specific Ab (α A) overnight. Then, goat anti-rabbit IgG (H + L) secondary Ab conjugated to horseradish peroxidase (HRP) was used (1:1,000 dilution), and the band was visualized using a DAB horseradish peroxidase color development kit.

2.5. Mouse immunization

Vaccine formulation was prepared by mixing TgERK7 (70 μ g/100 μ l sterile phosphate-buffered saline; PBS) in 100 μ l of Freund's adjuvant (FA) (Sigma, Missouri, USA). Freund's complete adjuvant (FCA) was used in the first two immunization doses and Freund's incomplete adjuvant (FIA) was used in three booster immunization doses. Each mouse in the vaccinated group ($n = 23$ mice) received 100 μ l of the adjuvanted recombinant protein (TgERK7 + FA) delivered via intramuscular (i.m.) injection and subcutaneously (s.c.) in the left and right posterior thighs and around the neck, weekly for 5 weeks. The control (PBS + FA) group ($n = 23$ mice) were injected in a similar manner, but with 100 μ l of PBS emulsified in the same Freund's adjuvants only without TgERK7. Mice in the third group ($n = 23$ mice) were left untreated (negative control). Further details of the vaccination schedules are summarized in Table 2.

2.6. Sample collection

Blood (300 μ l) was collected from the tail vein of three mice per group into a heparinized tube. Blood samples were collected prior to immunization and then at 2, 3, 4 and 6 weeks after the first immunization (Table 2). Collected blood samples were allowed to clot at 37 °C for 1 h, followed by the removal of clots by centrifugation at 500 xg for 10 min. Sera were stored at -20 °C until used for determination of total IgG Ab titers, anti-full length TgERK7 Ab titers, and TgERK7 peptide-specific Ab titers by an enzyme-linked immunosorbent assay (ELISA).

Two weeks post the final/fifth immunization, blood samples were collected from four mice per group to measure the level of cytokines induced after the completion of the immunization schedule (Table 2). Then, mice were euthanized by exposure to CO₂ and their spleens were harvested aseptically. A single-cell suspension of erythrocyte-free splenocytes was prepared by gently pressing the spleen through a 0.2 μ m mesh cell strainer. The splenocyte cultures were maintained in RPMI 1640 medium containing penicillin-streptomycin, sodium pyruvate, nonessential amino acids and 1% normal mouse serum.

2.7. Humoral responses

The total IgG Ab titers elicited by TgERK7 immunization in the mouse sera was determined in 96-well flat-bottom microtiter plates

using SBA Clonotyping™ System/HRP Kit (Southern Biotech, Birmingham, AL, USA) essentially as previously described (Li et al., 2014). We also examined whether the antibodies elicited by immunization would recognize each of the five TgERK7-specific peptides (Table 1) and the full-length TgERK7 protein. Briefly, 1 μ g of capture Ab provided in the kit, 1 μ g of each TgERK7 peptide, or equal amount of full-length TgERK7 protein expressed *in vitro* diluted in 100 μ l of PBS (pH 7.4) was adsorbed to the ELISA plate. The plate was washed with PBS containing 0.05 % Tween 20 (PBS-T) and blocked with PBS containing 1% bovine serum albumin (BSA) for 1 h. After blocking, 5 μ l of serum sample diluted with 95 μ l of PBS were added into the wells of plate and incubated for ~ 1 h at room temperature with gentle shaking. After washing, each well received 100 μ l of HRP conjugated anti-mouse IgG (1:250 dilution) and incubated overnight at 4 °C, and used for detection of the bound Abs. Binding was visualized by incubating with 100 μ l of substrate solution (pH 4.0) (0.03 % H₂O₂, 1.5 % ABTS, 1.05 % citrate substrate buffer). Absorbance was measured at 450 nm (OD₄₅₀) using ELISA reader (Bio-TekEL × 800, USA). All analyses were performed in triplicate, with appropriate positive and negative controls.

2.8. Cytokine detection

The concentrations of interferon-gamma (IFN- γ), interleukin 2 (IL-2), IL-4, IL-6, IL-10, IL-12p70, IL-23, monocyte chemoattractant protein-1 (MCP-1) and tumor necrosis factor-alpha (TNF- α) were measured in the sera obtained from four mice per group, two weeks after the final immunization dose (Table 2). Analysis was carried out using the LEGEND MAX™ Mouse ELISA Kits (Biolegend, San Diego, USA), as per the manufacturer's instructions. The minimum detection levels of the kits were: 8.0 pg/mL for IFN- γ , 0.9 pg/mL for IL-2, 0.5 pg/mL for IL-4, 2.0 pg/mL for IL-6, 2.7 pg/mL for IL-10, 0.5 pg/mL for IL-12p70, 4.8 pg/mL for IL-23, 3.5 pg/mL for MCP-1, and 1.5 pg/mL for TNF- α .

2.9. Flow cytometry measurement

The percentage of two subclasses (CD4⁺ and CD8⁺) of T lymphocytes in the single cell suspensions from mouse spleen was determined using flow cytometry, as previously described (Li et al., 2014). Briefly, cell viability was determined by 0.04 % trypan blue (Bio-Rad, California, USA) and 10⁶ viable cells were suspended in 100 μ l of PBS containing 2% fetal bovine serum (Invitrogen, California, USA). Cells were stained for 30 min at 4 °C in the dark with directly conjugated antibodies. Specifically, cells were stained using the following cell surface markers: phycoerythrin (PE)-labeled anti-mouse CD3e (5 μ g/mL), allophycocyanin (APC)-labeled anti-mouse CD4 (5 μ g/mL) and fluorescein isothiocyanate (FITC)-labeled anti-mouse CD8a (5 μ g/mL) antibodies according to the manufacturer's instructions (eBioscience, San Diego, USA). Lymphocytes were washed twice with PBS by centrifugation at 250 × g for 5 min and re-suspended in 300 μ l of

Table 2
Details of immunization schedules and parasite challenge studies in BALB/c mice.

Group	Treatments		Group size	Route of administration	Mice used in Ab analysis ^a	Mice used in T cell-mediated immunity analysis ^b	Challenged Mice (n)
	PBS/TgERK7	FCA/FIA					
Negative control	–	–	23	–	3	4	8 ^c , 8 ^d
PBS + FA	100 μ l	100 μ l	23	i.m. & s.c.	3	4	8 ^c , 8 ^d
TgERK7 + FA	70 μ g	100 μ l	23	i.m. & s.c.	3	4	8 ^c , 8 ^d

FA, Freund's adjuvant; FCA/FIA, Freund's complete/incomplete adjuvant; i.m., intramuscular injection in the thighs; s.c., subcutaneous injection around the neck.

^a Blood samples from three mice per group were collected from the tail vein prior to immunization and then at 2, 3, 4 and 6 weeks post the first immunization, to separate sera for determination of antibody (Ab) titers.

^b To investigate the serum cytokines and T lymphocyte subclasses in spleen, blood samples from four mice per group were collected from the tail vein; and spleens were aseptically removed, for preparation of erythrocyte-free single-cell suspensions 2 weeks post the final immunization.

^c Two weeks post the final immunization, 8 mice per group were intraperitoneally challenged with 1000 tachyzoites of *T. gondii* GT1 strain.

^d Two weeks post the final immunization, a further set of 8 mice per group were orally inoculated with 20 cysts of *T. gondii* PRU isolate.

fluorescein-activated cell sorter (FACS) buffer (PBS supplemented with 1% BSA + 0.1 % sodium azide), then fixed with 2% paraformaldehyde. Analysis was performed with a FACScan flow cytometer (Becton Dickinson, San Diego, CA) and data were analyzed using SYSTEM II software (Coulter).

2.10. Mouse challenge experiments

Two weeks after the final/fifth immunization dose, eight mice from each group were challenged intraperitoneally (i.p.) with 10^3 *T. gondii* GT1 tachyzoites per mouse, to test protection against acute infection. The mortality of mice was recorded daily, until all infected mice have died. Also, another set of eight mice per group were infected orally with 20 cysts of PRU strain. Four weeks post infection with PRU strain, brains of mice from vaccinated and non-vaccinated (control) groups were removed, and each brain was triturated in 1 mL of PBS. The number of cysts in 6–12 aliquots (20 μ l each) of brain suspensions was counted microscopically, and the average number of cysts was determined for each mouse. Further details of the challenge experiments are shown in Table 2.

2.11. In vitro replication of *T. gondii*

Two experiments were performed to investigate the inhibitory effect of the individually purified peptide-specific antibodies on the intracellular multiplication of *T. gondii*. In the first experiment, the purified antibodies were transfected into HFF cells using Pro-Ject™ Protein Transfection Reagent (Pierce Biotechnology, Illinois, USA). First, we examined the efficiency of transfection by measuring the antibodies in the transfected HFF cells. Briefly, transfected HFF cells were digested using 0.25 % trypsin (Transgen, Beijing, China) and a VCX750 ultrasonic processor (Sonics, Connecticut, USA). The supernatant was separated by centrifugation at $2000 \times g$ for 10 min, and the level of Ab subtypes (α A, α B, α C, α D and α E) was determined by ELISA assay - as described above. Cells transfected with an equal volume of serum-free medium (SFM) were used as a negative control. Next, HFF cells transfected with peptide-specific antibodies or SFM were cultured on coverslips (1×10^6 /well) in 24-well plates. The plates were incubated at 37 °C for 4 h, followed by washing three times with SFM. Cells were infected with *T. gondii* GT1 strain (10^6 tachyzoites in 1 mL of serum-containing medium) at a multiplicity of infection (MOI) of 1 (1 parasite to 1 host cell). In the second experiment, 10^6 tachyzoites were incubated with 500 μ l of SFM containing 60 μ g of each of the peptide-specific antibodies at 37 °C for 20 min. Ab-treated tachyzoites were then used to infect HFF cell monolayers in 24-well plate at MOI 1. For both experiments, the parasite intracellular proliferation was evaluated at 12, 24 and 36 h post infection (hpi). The number of tachyzoites per parasitophorous vacuole (PV) was counted by microscopy and at least 100 vacuoles were examined per sample. The parasites that have failed cytokinesis were counted as two, and PVs containing one tachyzoite at 36 hpi were not included in the count. The average from three independent experiments was determined. We further examined the early events of the parasite growth cycles (e.g., invasion and attachment of HFF cells) in order to identify which phase of the parasite infection cycle has been impacted by the anti-*T. gondii* activity of the peptide-specific Ab. This analysis involved the peptide A-specific Ab because it was the only Ab that showed significant inhibitory effect on the parasite proliferation compared to control. The invasion and attachment assays were performed using dual immunofluorescence assays (IFA) (α -TgSAG1 antibody prior to permeabilization and α TgGRA7 antibody after permeabilization) to allow the differentiation between extracellular and intracellular parasites, essentially as previously described in our recent work (Li et al., 2020).

2.12. Protein-protein interaction (PPI) analysis

To identify all protein interactions between putative TgERK7 and other proteins in *T. gondii*, we queried STRING Database using the function “protein by sequence search”, selecting *T. gondii* as organism and using *T. gondii*'s MAPK2 sequence as input (Szklarczyk et al., 2017). The resultant interactions were presented in a network using Cytoscape (Shannon et al., 2003). Next, we used protein BLAST program to identify human and mouse proteins that are most similar to TgERK7 sequence. Using the most TgERK7-homologous human and mouse proteins, we obtained the known interactions from the following databases: Intact (Orchard et al., 2014), String (Szklarczyk et al., 2017), BioPlex (Huttlin et al., 2017) and BioGrid (Chatr-Aryamontri et al., 2017). The resultant lists of interacting proteins were used to generate networks to show the interactions between TgERK7 homologous, and human and mouse proteins. To identify the functional annotations of the proteins involved in the PPI networks, we performed Gene Ontology (GO) enrichment analysis using FuncAssociate 3.0 (Berriz et al., 2003).

2.13. In silico modelling analysis

Structural information is unavailable for *erk7* and we generated initial conformations by homology modelling using I-TASSER and Phyre2 (Kelley et al., 2015; Zhang, 2008). The full-length *erk7* was not possible due to the lack of templates in the C-terminal part of the proteins. However, the N-terminal domain 1–351 has been characterized in orthologues, which provides suitable set of templates and we were able to generate a set of homology models with good reliability. The highest similarity orthologue was a MAP kinase *erk2* with a TM score of 0.485 and the top 10 ranked with TM score of 4.448 or higher (Zhang et al., 1994). All models agreed structurally with each other showing expected N-terminal variation due to reduced restraints.

The top N-terminal *erk7* 1–351 model from I-TASSER was prepared for MD simulations using CHARMM-GUI (Jo et al., 2008). In parallel, peptide *erk7* 3–14 was excised from the model and also prepared for MD simulations identically to the N-terminal in a water box with 12.5Å separation from each end of the putative protein/peptide in 150 mM KCl to isolate the Debye layers of the protein from images in the periodic boundary conditions. The systems were set up for simulations at 310 K using a CHARMM-36 force field. Equilibration under NVT and production runs under NPT restraints was carried out using NAMD 2.12 (Phillips et al., 2005). All equilibration runs were done on a U1 server with K80 and K40 Tesla GPUs while production was done in both vector mode on the U1 and using the scalar parallel architecture of the University of Nottingham HPC. Trajectory analysis and visualization were done using UCSF Chimera and VMD (Pettersen et al., 2004; Phillips et al., 2005).

2.14. Statistical analysis

Data collected from at least three independent biological replicates per experiment were analyzed using the SPSS Statistics 19.0 software package (SPSS Inc., Illinois, USA). The results are presented as the mean and standard deviation (Mean \pm SD). Differences in the data (e.g. Ab responses, cytokine production, flow cytometric analysis and *in vitro* parasite proliferation) between all the groups were examined by one-way ANOVA. (* $P < 0.05$, ** $P < 0.01$, and *** $P < 0.001$).

3. Results

3.1. Cloning and expression of putative TgERK7 protein

The pET-*erk7* plasmid was successfully constructed and induced to express recombinant putative TgERK7 protein. SDS-PAGE and Western blot analysis of the lysate prepared from *E. coli* BL21 (DE3) transfected with pET-*erk7* vector showed a single band with an estimated molecular

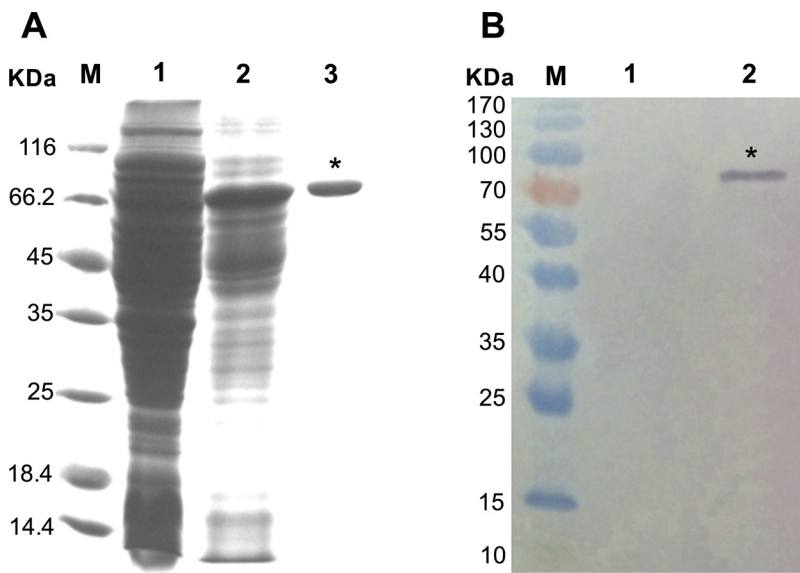


Fig. 1. *In vitro* expression and detection of TgERK7 protein. The putative TgERK7 protein was expressed in *E. coli* BL21 (DE3) strain and confirmed by (A) SDS-PAGE and (B) Western blot analysis. The rabbit anti-*T. gondii* TgERK7 peptide A-specific Ab (α A) was used as the primary Ab in the Western blot analysis. Only one band of \sim 74.4 kDa (indicated by asterisk) was detected in the lysate of pET-erk7-transfected cells, which was absent in the control cells transfected with empty pET-30a plasmid. Lanes: M, molecular mass (kDa) standard protein marker; 1, lysate prepared from *E. coli* BL21 (DE3) transfected with pET-30a empty vector; 2, lysate prepared from *E. coli* BL21 (DE3) transfected with the pET-erk7 vector; 3, lysate shown in lane 2 after purification using Ni-NTA His-Bind[®] Resin (Novagen).

mass of \sim 74.4 kDa (Fig. 1). However, no band of TgERK7 was detected in the lysate of bacterial cells transfected with the control pET-30a plasmid.

3.2. Total IgG, full length TgERK7 and peptide-specific Ab responses

Five antigenic peptides of TgERK7 protein were conjugated with KLH, and used to immunize rabbits for production of peptide-specific antibodies (α A, α B, α C, α D and α E, as shown in Table 1). The five TgERK7 peptides, the full-length TgERK7 protein expressed *in vitro* and the capture Ab provided in the ELISA kit were used to coat ELISA plate for detection of the levels of TgERK7-specific Abs (including full-length protein and five peptides) and total immunoglobulin G (IgG) titers in the serum samples collected at 0 (pre-immunization serum), 2, 3, 4, and 6 weeks after the first immunization. The level of anti-peptide A Ab in TgERK7 + FA-immunized mice was significantly increased compared with that of control mice, starting from three weeks post first immunization ($P < 0.05$) (Fig. 2A). Although some significant differences in the levels of the other four peptide-specific Abs were detected in the TgERK7 + FA-immunized group compared with the pre-immunization serum, these differences were not statistically significant when compared to PBS + FA immunized group (e.g. $P = 0.5282$ at 3 week, $P = 0.6624$ at 4 week, and $P = 0.1689$ at 6 week for anti-peptide B; $P = 0.2836$ at 3 week for anti-peptide C; $P = 0.4348$ at 2 week, and $P = 0.4306$ at 4 week for anti-peptide D; and $P = 0.5797$ at 4 week post the first immunization for anti-peptide E) (Fig. 2B-2E). Likewise, no significant difference was detected in the levels of anti-full-length TgERK7 or total IgG antibodies between immunized and non-immunized mice ($P > 0.05$) (Fig. 2F-2G). These results show that the effect of TgERK7 immunization on humoral response (total IgG, Abs against full-length TgERK7 and four peptides B, C, D and E) was comparable to the effect immunization using Freund's adjuvant only.

3.3. Cytokines induced by immunization

Levels of nine cytokines were determined in the sera of four mice from each group two weeks after the final immunization dose. The ELISA plates were read at 450 nm, and the absorbance was transformed to pg/mL using the calibration curves generated using the cytokine standards provided in the kits. The results showed that immunization elicited multifunctional T cell responses, where immune cells simultaneously produced a mixture of cytokines. As shown in Fig. 3, compared to the levels in the sera of negative control mice, eight cytokines in the sera of TgERK7 + FA-immunized mice were significantly elevated ($P =$

0.0054 for IFN- γ ; $P = 0.0152$ for IL-2; $P = 0.0142$ for IL-4; $P = 0.0007$ for IL-10; $P = 0.0304$ for IL-12p70; $P = 0.0018$ for IL-23; $P = 0.0473$ for MCP-1; and $P = 0.0119$ for TNF- α). Four of these cytokines were also significantly increased in the mouse group injected with PBS + FA compared to negative control ($P = 0.0013$ for IL-10; $P = 0.0474$ for IL-12p70; $P = 0.0258$ for IL-23; and $P = 0.0198$ for TNF- α). In comparison to the PBS + FA group, concentrations of six cytokines were elevated in the TgERK7 + FA-immunized group ($P = 0.0316$ for IFN- γ ; $P = 0.0492$ for IL-2; $P = 0.0134$ for IL-4; $P = 0.0229$ for IL-10; $P = 0.0064$ for IL-23; and $P = 0.0195$ for TNF- α) (Fig. 3). No significant difference was detected between TgERK7 + FA-immunized group and PBS + FA group for IL-6, IL-12p70 or MCP-1 ($P > 0.05$).

3.4. TgERK7 induced CD3e⁺CD4⁺ T lymphocytes in spleen

We investigated whether the putative TgERK7 protein can induce T lymphocytes in the mouse spleen two weeks after the final immunization dose. The subclasses of T lymphocytes (CD3e⁺CD4⁺ T cell and CD3e⁺CD8a⁺ T cells) in single-cell suspensions obtained from spleen of four mice per group were examined using flow cytometry. The number of CD3e⁺CD4⁺ T cells were significantly higher in the (TgERK7 + FA)-immunized mice (%: 5.38 ± 1.57 , $P = 0.0211$), when compared to mice in the negative control group (%: 0.48 ± 0.13). However, no difference was detected between mice vaccinated with TgERK7 + FA ($P = 0.3225$) and mice vaccinated with PBS + FA (%: 10.43 ± 4.16) (Fig. 4A, 4C). In regard to CD3e⁺CD8a⁺ T lymphocytes, no difference was detected between the negative control mice (%: 4.43 ± 0.45) and mice treated with TgERK7 + FA (%: 3.90 ± 0.09 , $P = 0.2962$) or PBS + FA (%: 5.60 ± 0.21 , $P = 0.0561$). However CD3e⁺CD8a⁺ T cells in TgERK7 + FA group were significantly decreased compared to mice vaccinated with PBS + FA ($P = 0.0017$) (Fig. 4B, 4D). Compared with negative control mice (0.11 ± 0.04), the ratios of CD3e⁺CD4⁺ T/CD3e⁺CD8a⁺ T in (TgERK7 + FA)-immunized mice (1.38 ± 0.42 , $P = 0.0232$) were significantly increased; however there was no difference between the PBS + FA group (1.80 ± 0.69 , $P = 0.0922$), and mice in the two other groups ($P = 0.6280$) (Fig. 4E).

3.5. Anti-*T. gondii* effect of TgERK7peptide- specific Abs

We examined the anti-*T. gondii* activities of five peptide-specific antibodies on the intracellular proliferation of *T. gondii* by incubating the parasite with each Ab prior of infection or by infecting host cells that have been already transfected with Ab. The efficiency of Ab transfection was confirmed using ELISA as shown in Fig. 5A. The effect

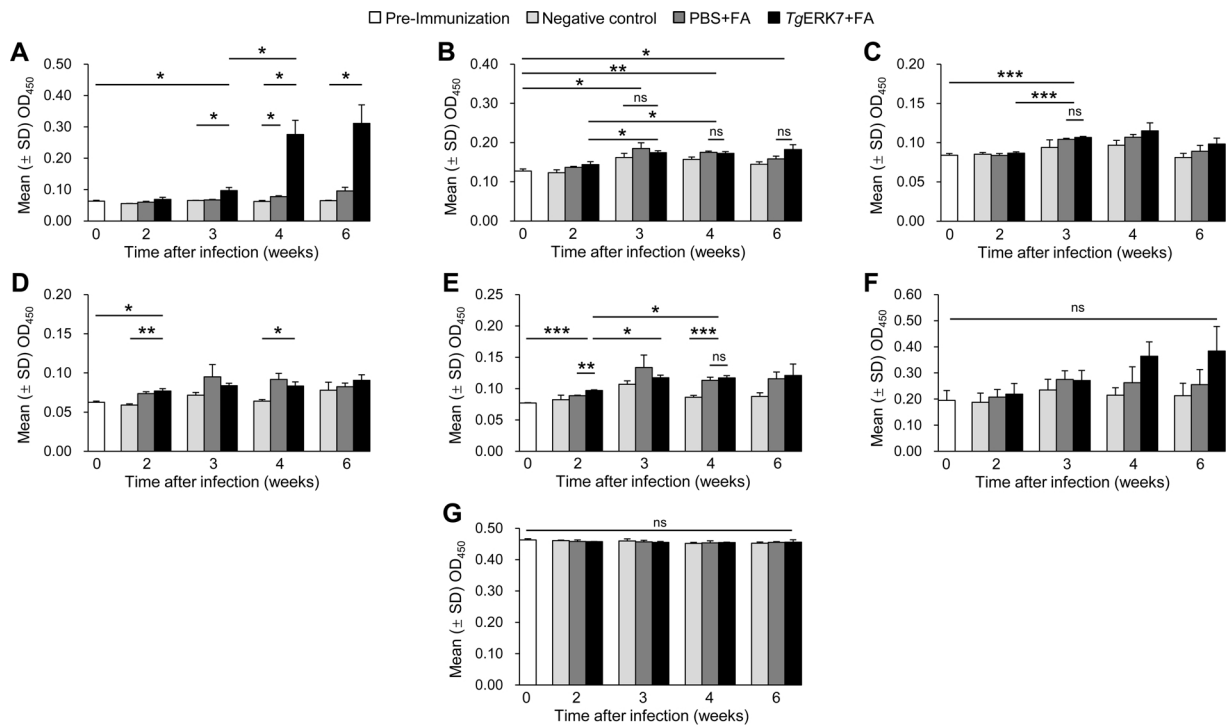


Fig. 2. Antibody (Ab) responses after five immunization doses using putative *TgERK7* protein. Levels of specific antibodies against (A) *TgERK7* peptide A, (B) *TgERK7* peptide B, (C) *TgERK7* peptide C, (D) *TgERK7* peptide D, (E) *TgERK7* peptide E, (F) full-length putative *TgERK7*, and (G) total IgG were determined at OD₄₅₀. Ab titers were determined in the sera of *TgERK7* +FA-immunized group and control (PBS + FA-treated and untreated negative control) groups ($n = 3$ /group) at 0 (pre-immune serum), 2, 3, 4, and 6 weeks after the first immunization. The anti-*TgERK7* peptide A antibodies progressively increased over the course of the immunization period. Data points represent the mean values, with error bars indicating the standard deviations. ns, not significant; *, $P < 0.05$; **, $P < 0.01$; ***, $P < 0.001$. FA indicates Freund's adjuvant.

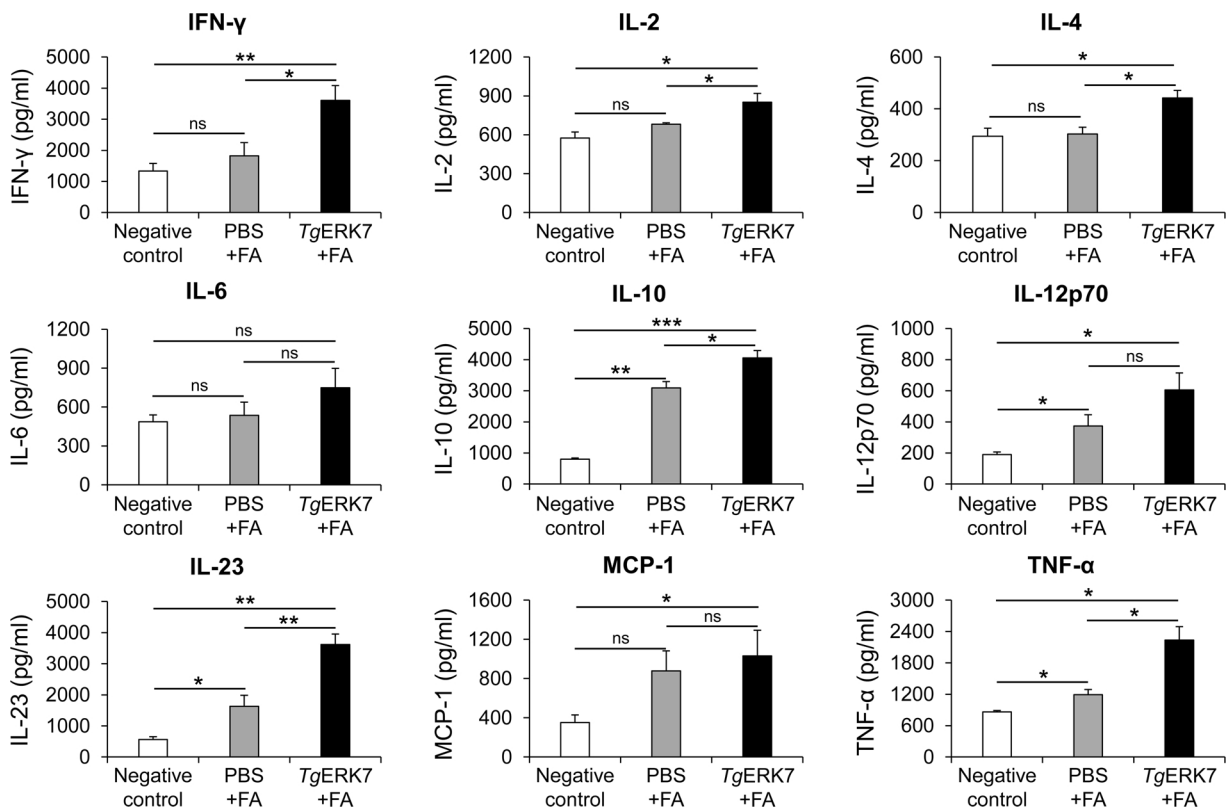


Fig. 3. *TgERK7* immunization induced serum cytokines in immunized mice. The concentrations of nine cytokines (IFN- γ , IL-2, IL-4, IL-6, IL-10, IL-12p70, IL-23, MCP-1, and TNF- α) in the mouse serum were determined by ELISA. ANOVA analysis of the data show that the cytokine concentrations at 2 weeks after the final immunization were significantly higher than that of control mice. Standard deviations are indicated by error bars. ns, no significant difference; *, $P < 0.05$; **, $P < 0.01$; ***, $P < 0.001$. FA denotes Freund's adjuvant.

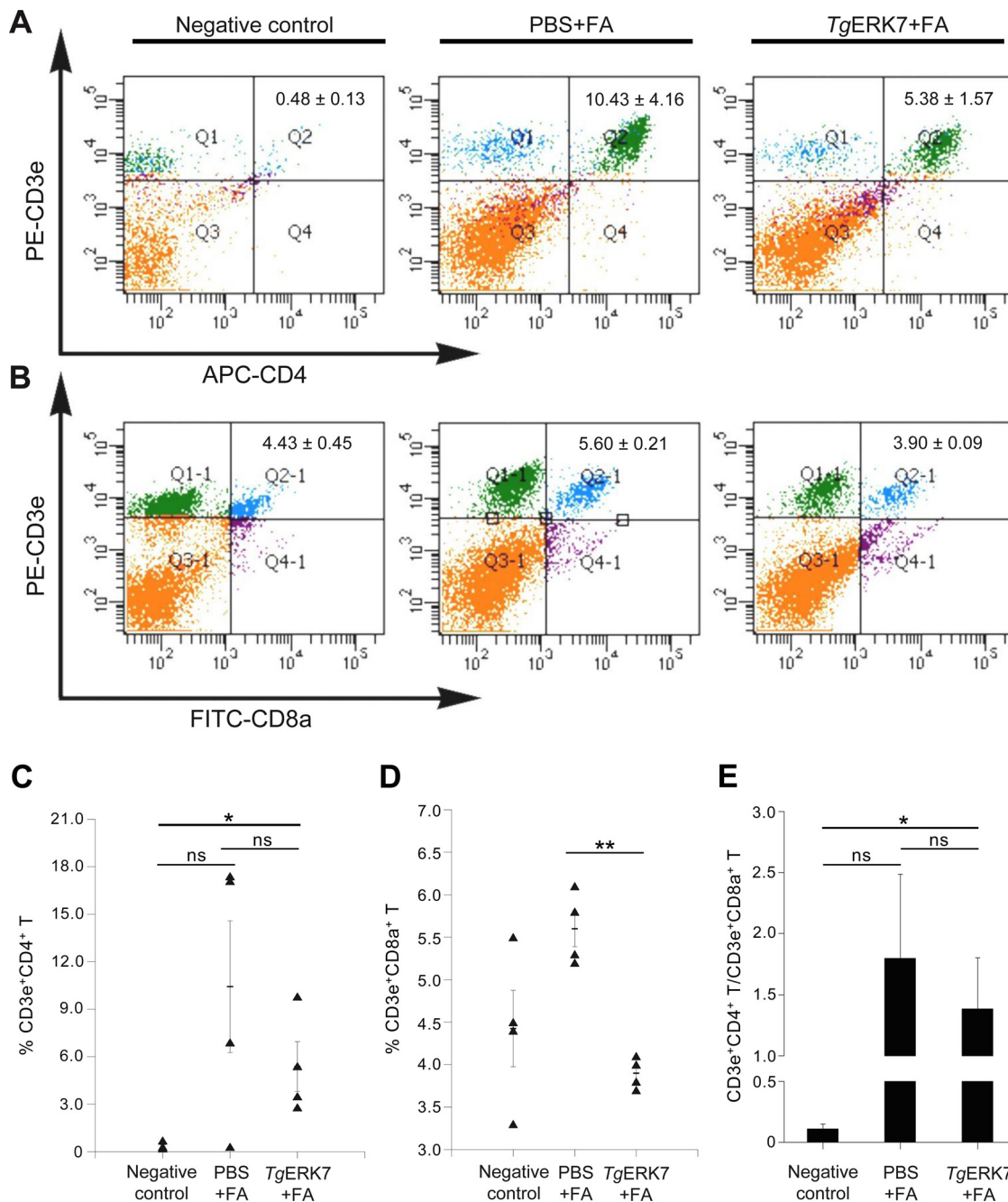


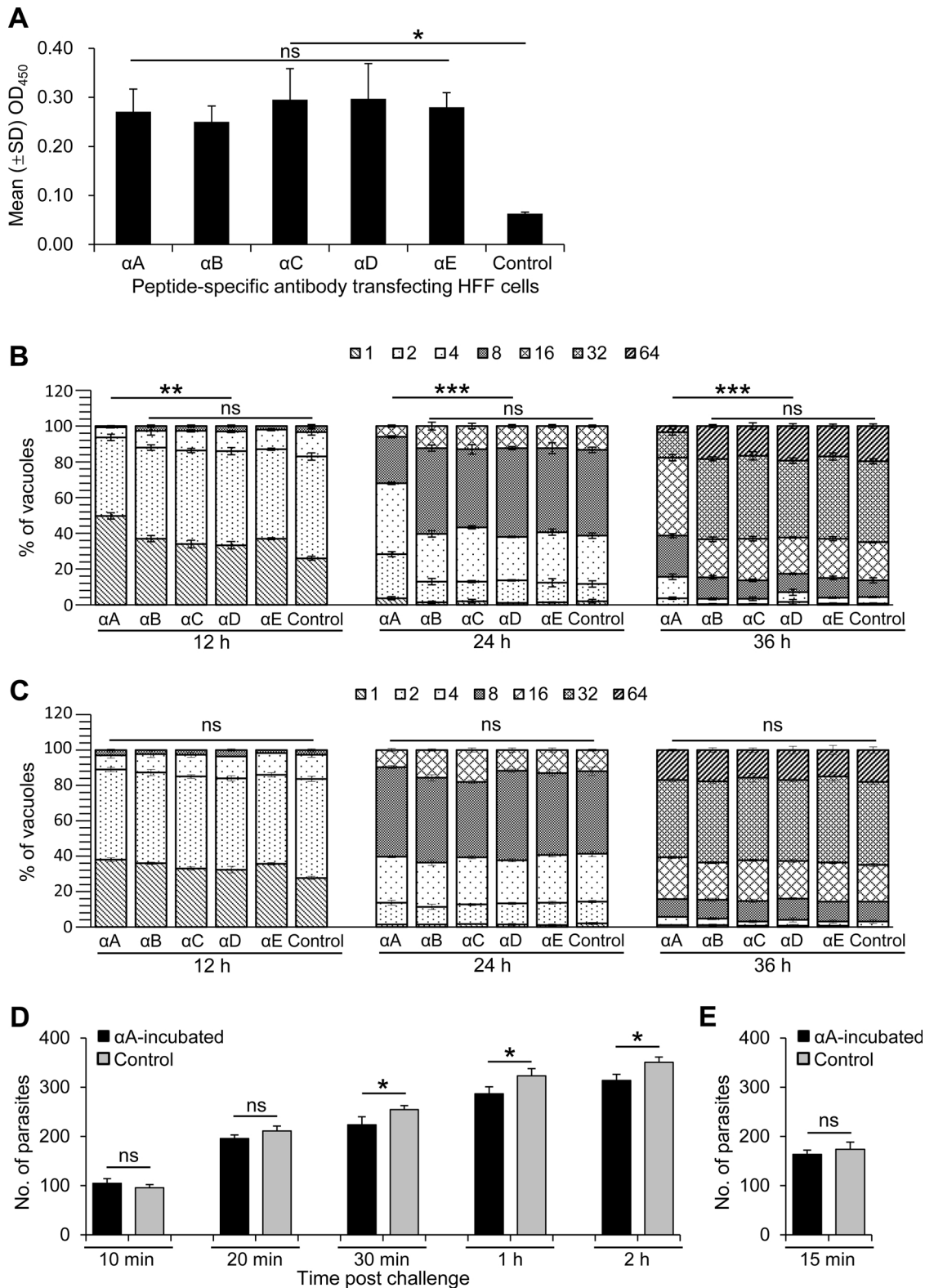
Fig. 4. The levels of T lymphocyte subclasses in spleen of mice 2-weeks post the final immunization dose with the putative TgERK7 analyzed using flow cytometry. (A) CD3e⁺CD4⁺ T and (B) CD3e⁺CD8a⁺ T lymphocytes (mean ± SD) were distributed in the regions Q2 and Q2-1, respectively. The percentages of (C) CD3e⁺CD4⁺ T and (D) CD3e⁺CD8a⁺ T cells in single-cell suspensions of splenocytes of mice two weeks after the final immunization. Responses from individual mice are indicated using black triangles. (E) The ratio between CD3e⁺CD4⁺ T and CD3e⁺CD8a⁺ T cells. ns, not significant; *, $P < 0.05$; **, $P < 0.01$. FA indicates Freund's adjuvant.

of treatment with different Abs on the intracellular proliferation of *T. gondii* GT1 tachyzoites within HFF cells was investigated at three time points (12, 24 and 36 h) after infection. Compared to the control, significant delay in the proliferation of *T. gondii* was detected when the parasite was incubated with anti-peptide A Ab prior to infection ($P = 0.0025$ at 12 h; $P = 0.00016$ at 24 h; and $P = 6.3 \times 10^{-11}$ at 36 h) (Fig. 5B). There was no difference between the other four peptide-specific Abs (α B, α C, α D, α E) and the control. Likewise, no difference in the parasite growth was detected between HFF cells transfected by any of the five peptide-specific Abs and control HFF cells ($P > 0.05$) (Fig. 5C). Prior incubation of tachyzoites with α A significantly reduced the invasion of *T. gondii* from 30 min onwards in a time-dependent

manner ($P < 0.05$; Fig. 5D). However, there was no significant difference in the parasite attachment at 15 min post infection between α A-treated group and control ($P > 0.05$; Fig. 5E). Based on these results, we conclude that α A inhibits the intracellular proliferation of *T. gondii* most likely *via* delaying the parasite's invasion.

3.6. Successive immunizations protect mice against acute *T. gondii* infection

TgERK7-immunized and non-immunized (control) mice were challenged with 10^3 tachyzoites of *T. gondii* GT1 strain (Genotype I) or 20 cysts of PRU isolate (Genotype II), two weeks after the final immunization. The data showed that survival times of TgERK7+FA-



(caption on next page)

immunized mice (13.8 ± 3.4 d) were significantly higher, when compared with the control mouse groups (9.1 ± 0.7 d, $P = 0.0040$ for PBS+FA group; 9.5 ± 2.2 d, $P = 0.0066$ for negative control group). No significant difference was detected in the mouse group treated with PBS+FA (9.1 ± 0.7 d) when compared with mice in the negative control group ($P = 0.6372$). All infected mice had died within 19 days

post challenge (Fig. 6A). The mortality rates of mice infected with PRU cysts 15 days post challenge were 4/8 (50 %) in mice immunized by TgERK7+FA, 2/8 (25 %) in mice immunized by PBS + FA, and 8/8 (100 %) in the negative control mice. There was no significant difference in the survival times between the negative control mice (12.0 ± 0.5 d) and mice immunized by TgERK7+FA (11.0 ± 0.4 d, P

Fig. 5. Exposure of *T. gondii* tachyzoites to TgERK7 peptide A-specific antibody (Ab) prolonged their intracellular replication. (A) ELISA assay was used to confirm the efficiency of transfection of peptide-specific Abs. Optical densities of HFF cells transfected with each of the five peptide-specific Abs were higher compared to control HFF cells transfected with serum-free medium (SFM) only ($P = 0.0111$ for αA ; $P = 0.0045$ for αB ; $P = 0.0213$ for αC ; $P = 0.0312$ for αD ; and $P = 0.0020$ for αE). No significant difference was detected between any two of HFF cells transfected with peptide-specific Abs ($P > 0.05$), showing the success of the Ab transfection. The purified peptide-specific Abs were co-incubated with *T. gondii* GT1 tachyzoites (B) or transfected into HFF cells (C) prior to the infection and the level of parasite proliferation was examined. The data show that *T. gondii* co-incubation with peptide A-specific A (αA) prolonged the intracellular proliferation of this parasite. However, this observation was not detected when the parasite was incubated with Abs specific to any of the other 4 peptides (B, C, D and E) nor in HFF cells transfected with any of the 5 peptide-specific Abs. The early events of *T. gondii* growth cycle, invasion (D) and attachment (E), were further analyzed by IFA using $\alpha TgGRA7$ and $\alpha TgSAG1$ Abs. (D) Invasion of *T. gondii* tachyzoites incubated with αA was significantly delayed starting from 30 min post infection compared to control tachyzoites incubated with SFM prior to infection ($P < 0.05$). (E) There was no difference in the attachment of tachyzoites at 15 min between αA -treated and SFM-treated tachyzoites. These results suggest that αA -mediated reduction in the parasite proliferation is attributed to reduction in the parasite invasion. ns, not significant; *, $P < 0.05$; **, $P < 0.01$; ***, $P < 0.001$.

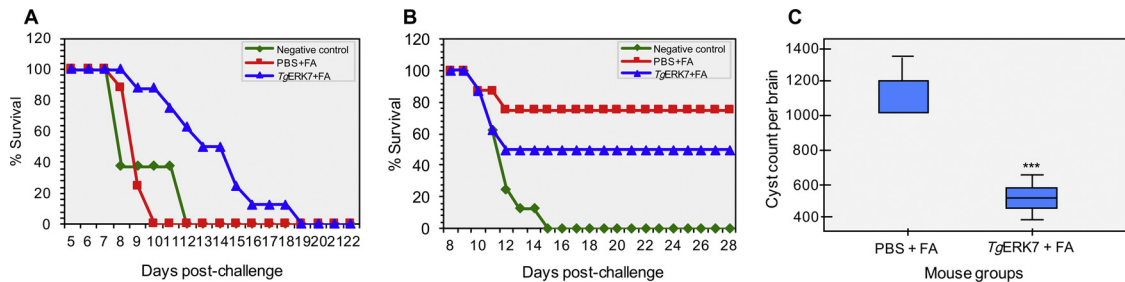


Fig. 6. Five immunization doses with putative TgERK7 protein protected mice against acute infection and reduced brain cyst burden. (A) Survival of BALB/c mice after intraperitoneal challenge with 10^3 tachyzoites of *T. gondii* GT1 strain 2-weeks after the fifth immunization dose. The survival time of TgERK7-immunized group (13.8 ± 3.4 d) was significantly increased compared to the two control groups (9.1 ± 0.7 d for PBS + FA and 9.5 ± 2.2 d for the negative control) ($P < 0.01$). (B) Survival of the immunized mice following oral infection with 20 cysts of PRU strain 2-weeks after the fifth immunization dose. No significant difference was detected between TgERK7-immunized group and PBS + FA-immunized group ($P > 0.05$). (C) The number of *T. gondii* cysts in the brain of the survived mice four weeks post challenge. The brain cyst number of TgERK7-immunized mice (500 ± 40.8) was significantly reduced, compared with that of the control PBS + FA-immunized group (1166.7 ± 61.5) (***) ($P < 0.001$). Standard deviations are indicated by error bars. FA indicates Freund's adjuvant.

= 0.2515) or mice immunized with PBS + FA (11.0 ± 1.0 d, $P = 0.4236$) (Fig. 6B). However, the number of brain cysts in the survived TgERK7 + FA-immunized mice (500.0 ± 40.8 , $P = 0.00004$) was significantly reduced ($P < 0.001$) when compared with the control group (PBS + FA: 1166.7 ± 61.5) at four weeks post challenge with PRU cysts (Fig. 6C). These results suggest that successive immunizations with putative TgERK7 protein can enhance the survival of acutely infected mice and significantly reduce the brain cyst burden in mice with chronic *T. gondii* infection.

3.7. Protein-protein interaction networks

Using STRING Database, we identified 26 *T. gondii* protein interactions (Fig. 7A), having TgMAPK2, as the most homologous protein in the database, based on *T. gondii* sequence. The functional annotation of proteins involved in this parasite-parasite protein interaction network is

shown in Table S1. TgERK7-homologous (TgMAPK2) seems to interact with proteins of the rhoptyry kinase family (ROP7, ROP21, ROP31, ROP35). The finding that TgERK7 interacts with protein serine/threonine phosphatase (PSTP) (Uniprot Id: B9QE64) was interesting because PSTP plays a role in the regulation of MAPK signaling. However whether or to what extent PSTP influences the phosphorylation of TgERK7 remains to be determined.

BLAST search identified MAPK15 (Uniprot Id: Q8TD08), which is also known as ERK7, as the human protein that is most closely related to TgERK7. Both TgERK7 and MAPK15 have sequence similarity values of a E-value of $5e-129$, a query cover of 64 %, and a total score 395. Using the MAPK15 protein as input to query the interaction databases (Intact, String, BioPlex, and BioGrid), we obtained 25 pairwise protein interactions with 21 human proteins (Fig. 7B). MAPK15 seems to have bidirectional relationship with PCNA, CLIC3 and MAP1LC3B. The GO enrichment analysis revealed that these 21 proteins are most

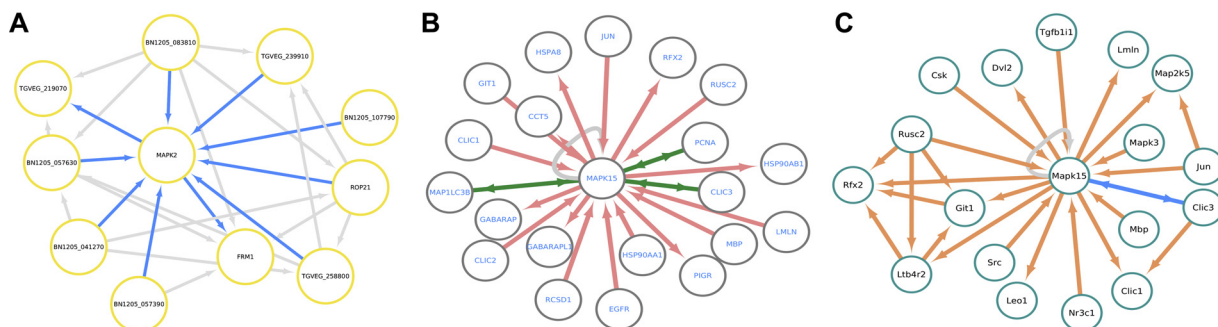


Fig. 7. Protein-protein interaction networks. (A) Interaction of putative TgERK7 protein with other *T. gondii* proteins. MAPK2 represents the most homologous protein to TgERK7 sequence. Blue arrows represent the principal interactions of MAPK2 node, whereas gray arrows denote second level interactions. (B) Human (*Homo Sapiens*) protein interactions having MAPK15 (Uniprot Id: Q8TD08), the human homologous of *T. gondii* sequence, as an initial node. Red arrows represent unidirectional relationship, whereas green arrows represent bidirectional relationship and the gray arrow represents an auto-relation. (C) Mouse (*Mus Musculus*) protein interactions having MAPK15 (Uniprot Id: Q80Y86) is the murine homologous of TgERK7. Orange arrows represent unidirectional relationship, whereas blue arrows represent bidirectional relationship and the gray arrow represents a self-relation.

significantly enriched in chaperone-mediated autophagy, nitric-oxide synthase regulator activity, MHC class II protein complex binding, DNA polymerase binding, and MHC protein complex binding. The full results of functional annotation of interacting human proteins are shown in Table S2.

BLAST search also revealed that *Mus musculus* MAPK15 (Uniprot Id: Q80Y86) is the most closely related to TgERK7, having a E value of 4e-133, a query cover of 57 % and a total score of 405. Using MAPK15 protein to obtain all known interactions with *M. musculus* proteins, we obtained 28 interactions with 18 mouse proteins (Fig. 7C). The GO enrichment analysis showed that the most relevant biological functions of these interacting proteins are regulation of telomerase activity, regulation of telomere maintenance via telomerase, regulation of telomere maintenance via telomere lengthening, positive regulation of DNA biosynthetic process, and focal adhesion. The full results of functional annotation of these interacting mouse proteins are shown in Table S3.

3.8. Computational modelling of the ERK7 putative protein

High performance computing approaches offer detailed insights into the molecular mechanisms underpinning experimental observations of genetic and phenotypic variations (Sloan et al., 2019). To understand the molecular and structural differences that confer enhanced antigenicity to pep1 in solution in comparison to the same sequence as 3–14 part of *erk7* we carried out MD simulations of the peptide A alone and of the N-terminal fragment of *erk7* 1–351. We hypothesise that a free peptide offers unrestricted antigen presentation in comparison to the same sequence participating in the protein fold of *erk7*, where it is sheltered by neighbouring motifs. Further to that, we propose that the peptide in solution is structurally less restrained and can complement an antibody challenge better than when embedded as a component of the structured N-terminal *erk7*.

In the absence of structural data on *erk7*, homology modelling was used to generate lead conformations for the protein and the isolated peptide. The lead model from I-TASSER was selected for MD simulations to anneal the models and remove residual conformational strain inherited from modelling templates. Structure annealing was complete within 100 ns of simulations for the N-terminal domain of *erk7* 1–351 and within 50 ns for pep1, where in both cases structural drift had subsided in the late stages of the simulations and only stochastic noise modulated a steady RMSD average (Fig. 8A).

To understand the conformational variation of the peptide backbone within the protein and compare it to free peptide in solution we used conformational cluster analysis over the periods of simulations. Conformational clusters report metastable structural intermediates of a molecular system during the time evolution of its structure, which can interconvert and contribute to the dynamically averaged structure observed after computational evolution is complete. Fig. 8B shows aligned conformations from the top four clusters of the peptide *erk7* 4–13 as part of the N-terminal domain *erk7* 1–351 along with end of trajectory conformation. Structural members of the most populated clusters show good conformational agreement with each other over the entire trajectory, which shows that the peptide structure is stable within its *erk7* cleft.

Despite this well-defined conformation as part of *erk7*, the peptide 3–14 shows some dynamic freedom compared to the rest of the protein and undergoes transient excursions outside its cleft. At the start of the MD trajectory the peptide *erk7* 4–13 was set into a groove of the N-terminal domain *erk7* 1–351 following the homology model built on similarity to a crystalline orthologue. Comparatively early in the evolution, the N-terminus was freed from the groove in the protein domain and continued evolving in an exchange process in transient contacts with the rest of the domain (Fig. 8C). Such conformational excursions present the peptide for IGG binding, which is hindered when the peptide is nested into a protein groove. This explains why the peptide does show some antigen activity even as part of the *erk7* protein.

In contrast to peptide *erk7* 4–13, the conformation of pep1 in solution is quite fluid and structural alignment shows significant conformational variations between the top four clusters (Fig. 8B). Besides its greater conformational flexibility, the mean conformation of pep1 appears more closed with a reduced end-to-end distance. This is illustrated in the end-to-end radial distribution function (RDF), which reflects the fraction of time along the MD trajectory that the α -carbons of the two end residues of the peptide spend a given distance apart (Fig. 8D). In that regard the free peptide behaves as an intrinsically disordered system with end-to-end distance primarily in the region of 9–10 Å but undergoing excursions from approximately 5 Å to nearly 28 Å. By contrast, the peptide *erk7* 4–13 as part of the N-terminal domain of *erk7* 1–351 is structured with tightly clustered end-to-end distances around 15 Å. The functional consequence of this difference is that the free peptide is flexible and accessible for binding invitations from IGG and can respond to conformational variations as an intrinsically disordered protein. This explains its higher antigenicity compared to the same sequence presented as part of *erk7* (Dyson and Wright, 2005) where peptide *erk7* 3–14 with N-terminal *erk7* is sheltered with only transient antigen presentation.

4. Discussion

The objective of this study was to produce a recombinant TgERK7 protein and to examine its potential as a vaccine to improve the protective responses against *T. gondii* infection in BALB/c mice. Generating balanced Th1 and Th2 immune responses is necessary for limiting *T. gondii* proliferation, while in the meantime protecting the host from severe inflammatory pathologies (Lüder and Rahman, 2017). Therefore, we examined the serum levels of total anti-*T. gondii* IgG antibodies, and antibodies produced against the full-length TgERK7 protein and against five specific TgERK7 peptides. We also determined the concentrations of nine serum cytokines and the levels of T lymphocyte subclasses in the spleen of immunized mice. We were interested in finding out how immunization with TgERK7 protein can influence these factors, which play important roles in mediating host response to *T. gondii* infection (Fallahi et al., 2018; Rougier et al., 2017; Sasai et al., 2018).

First, we determined the total IgG titers and full-length TgERK7-specific Ab responses in mice following immunization with a recombinant TgERK7 protein using ELISA. Immunization with TgERK7 did not significantly alter the levels of total IgG titers or anti-full-length putative TgERK7 Abs in the immunized mice compared to non-immunized (control) mice. We also used ELISAs to determine the reactivity of five TgERK7-derived peptides to the sera of the immunized mice and to reveal differences in Ab specificities in the post-immunization sera. Interestingly, Ab titers against TgERK7 peptide A significantly increased in the sera of immunized mice compared to Ab titers prior to immunization. Multiple immunizations in mice were necessary to induce peptide A-specific Ab response of a significant magnitude. This demonstrates that antigen-specific humoral immune responses elicited following recombinant TgERK7 protein immunization is driven by TgERK7 peptide A, which may not have been sufficient to trigger a strong humoral response.

Cytokine analysis showed that cytokines such as IFN- γ and IL-12p70, which play key roles in the protection against *T. gondii* infection, were induced by successive immunizations with TgERK7 protein. *T. gondii* induces a type 1 response mediated by the production of proinflammatory cytokines, such as IFN- γ by T cells and natural killer cells to control acute infection caused by the rapidly proliferating tachyzoites (Kamiyama and Hagiwara, 1982; Rytel and Jones, 1966). While cell-mediated immunity is critical for the effective control of *T. gondii* infection, the attenuation of the inflammatory response is also important to ensure the maintenance of immune homeostasis, while limiting immune pathology. In a previous study, IL-10-deficient C57BL/6 mice exhibited elevated IL-12 levels, and increased TNF- α and IFN- γ

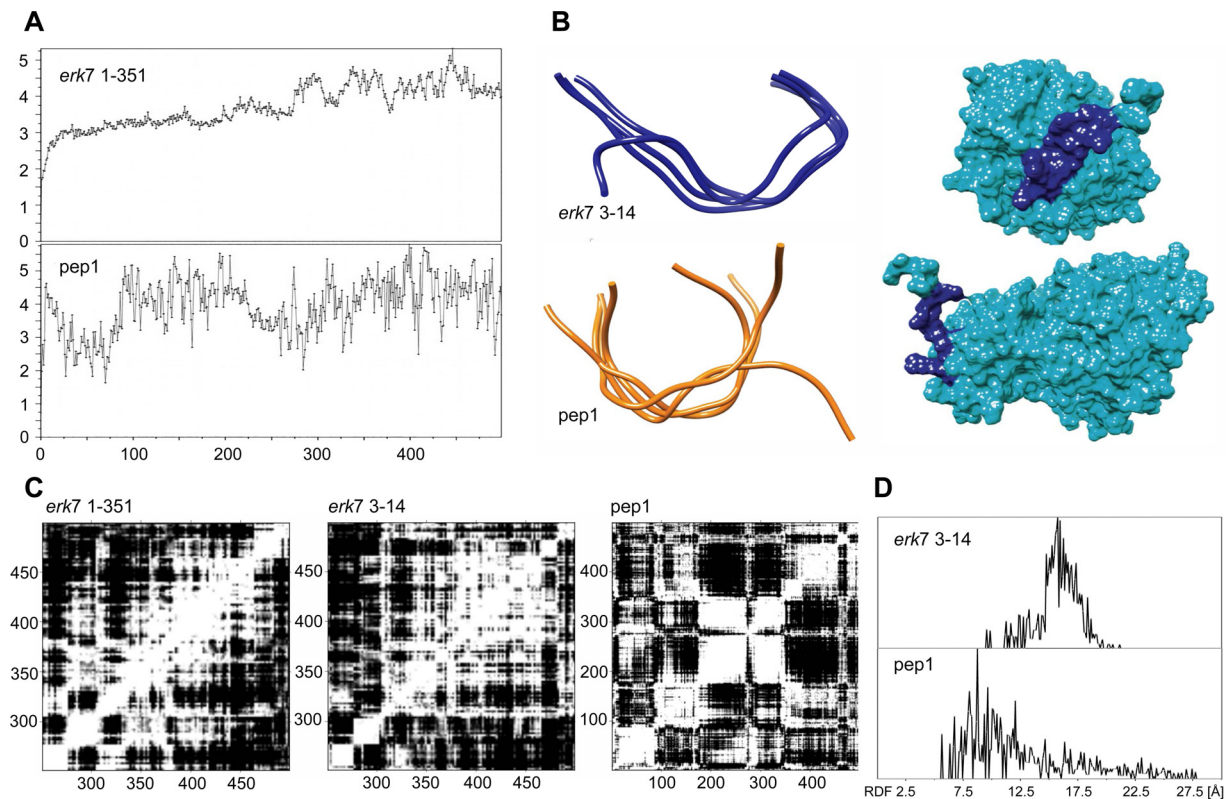


Fig. 8. (A) Root mean square deviation, RMSD, in Å for N-terminal *erk7* 1-351 (top, 100 ns) and pep1 (bottom, 50 ns). Annealing of N-terminal *erk7* 1-351 ends around frame 350/500 or 70 ns, while the small pep1 anneals very quickly within the first few tens of ns. RMSD is constrained within approximately 1 Å across the entire protein for N-terminal *erk7* 1-351, while RMSD readily fluctuates within 2 Å in the free peptide. (B) Aligned average backbone conformations from top four clusters for *erk7* 3-14 (top left, blue) and pep1 (bottom left, orange). The peptide shows much better defined structure as part of the N-terminal *erk7* 1-351 fragment but is very flexible in solution allowing it to respond to binding requests from conformationally dissimilar epitopes as an intrinsically disordered peptide. The location of *erk7* 3-14 within the N-terminal domain *erk7* 1-351 is shown on the right from the last frame of 100 ns trajectory in blue with the rest of the protein shown in cyan. (C) Frame-to-frame RMSD over the trajectory. Evolution of backbone conformation defines conformational clusters: N-terminal *erk7* 1-351, last 50 ns (left); *erk7* 4-13, last 50 ns (middle); pep1, 50 ns (right). White shows low variation and black shows “hot” regions or significant changes in RMSD. The intensity maps range from 1.3 to 4.8 Å for *erk7* 1-351 (left) through 0.9 to 5.7 Å for *erk7* 4-13 (middle) to 0.8 to 10.2 Å for pep1 (right). (D) Pairwise radial distribution function, RDF, between the α -carbons of residues 4 and 13 in *erk7* 4-13 (top) and between α -carbons of residues 1-9 in pep1 (bottom) over 100 and 50 ns trajectories. The peptide conformation within N-terminal *erk7* 1-351 is well-defined with tightly clustered end-to-end distance around 15 Å, while the free peptide is intrinsically disordered with end-to-end distance primarily in the region of 9-10 Å but undergoing excursions from approximately 5 Å to nearly 28 Å.

responses, resulting in severe inflammatory pathologies (Gazzinelli et al., 1996). Therefore, increased IL-10 level in our study may function to balance the high IFN- γ response in mice following *T. gondii* infection. The Th2-type cytokine IL-10 favors an attenuation of host defense mechanism against *T. gondii* invasion, by restraining Th1-mediated inflammatory response, while maintaining a Th2 immune response (Thouvenin et al., 1997). This balanced immune response seems to protect the host and offers a supportive environment for the establishment of latent infection (Denkers and Gazzinelli, 1998).

T cells, major histocompatibility complex (MHC) class I-restricted CD8⁺ T cells and MHC class II-restricted CD4⁺ T cells, are required for protective immunity against *T. gondii* infection; and play key roles in infection resolution and protection against reinfection (Gazzinelli et al., 1992; Suzuki and Remington, 1988). CD8⁺ T cells have the capacity to remove cysts from the brain of chronically infected mice (Ochiai et al., 2016; Suzuki et al., 2010). Mice that lack T cells do not survive to the chronic stage of infection, and depletion of T cells resulted in reactivation of tissue cysts (Gazzinelli et al., 1992; Hunter et al., 1994). In our study, the level of CD4⁺ T cells, but not CD8⁺ T cells in mouse spleen was significantly induced by *Tg*ERK7 immunization. The decreased induction of CD8⁺ T lymphocyte may be related to the protein used in immunization; even with FA boosting *Tg*ERK7 protein was not good enough at eliciting a cytotoxic T cell response. It is intriguing that

the induction of CD8⁺ T cell was poor, but the vaccine still managed to prolong the survival of mice after challenge with the virulent GT1 strain (Genotype I) and also caused ~ 50 % reduction in brain cyst burden post challenge with the PRU strain (Genotype II). It remains paradoxical to observe a significant decrease in the parasite burden in the brain of immunized mice challenged with *T. gondii* PRU strain, despite the lack of enhanced CD8⁺ T cell response.

When the inhibitory effect of α A on *T. gondii* growth *in vitro* was investigated we found that asexual replication of *T. gondii* within HFF cells was significantly prolonged when the parasite was incubated with α A prior to infection. However, neither treatment with any of the antibodies specific to any of the other four peptides (α B, α C, α D, α E) nor transfecting cells with any of the five peptides showed any inhibitory effect on *T. gondii* growth. These results suggest that inhibition of the parasite growth was mediated by α A response, likely *via* impairment of the biological functions of certain components that play a role in the invasion and/or growth of *T. gondii*. As discussed above, although *Tg*ERK7 immunization did not elicit high levels of total IgG, anti-full-length *Tg*ERK7 Abs or specific Abs to the four peptides (B, C, D and E), immunization induced a high level of anti-peptide A Abs. Also, our results showed increased CD3e⁺CD4⁺ T lymphocyte proportion in spleen of immunized mice. These results provide more evidence to support the hypothesis that Abs produced against peptide A

(DEVDKHVLRLKYD) by TgERK7 immunization might have neutralized the tachyzoite's ability to invade and/or colonize host cells. Therefore, it is likely that the protective effect of anti-peptide A Ab in acutely infected and immunized mice may be attributed to α A-mediated neutralization of functional key ERK7 peptide epitope(s). This humoral immune response also seems effective for controlling the parasite during chronic infection.

The finding that multiple immunizations induced only peptide A-specific Ab response of a protective magnitude was unexpected. Therefore, we attempted to reflect on the potential reasons as to why Ab against peptide A seems to have the most potent anti-*T. gondii* activity. Antigen presentation is described traditionally through crystal structures of antigen/Ab fragments that are frozen in time. The process of recognition, however, is more complex and is guided by long-range interactions, diffusion and segmental dynamics of both partners (Abriata and Dal Peraro, 2015; Bretou et al., 2016). The dynamic picture presented in the MD simulations emphasizes the importance of accessibility and flexibility of a simple antigen sequence (peptide A in this case). The observed conformational flexibility of the N-terminal peptide when liberated from the restrictions of a protein crustal explains its antigenicity and capacity to engage the antibody. Taking the step further and releasing the sequence from its anchor point into a free, disordered structure, markedly enhances its antigenicity and adaptability to meet the conformational expectations of antibodies.

It would be important to understand why blocking ERK7 leads to inhibition of the parasite invasion *in vitro* and protected mice against acute and chronic infections. In *T. gondii*, two MAPK orthologs, designated as MAPK1 and MAPK2, have been shown to play roles in host-cell attachment, bradyzoite differentiation and parasite replication (Cao et al., 2016; Li et al., 2016). Severe developmental defects have been described in *T. gondii* deficient in MAPK1 (Cao et al., 2016). Also, deletion of MAPK1 and MAPK2 in *T. gondii* type I tachyzoites rendered the mutant strains less virulent in mice. Also, mice infected with mutant strains exhibited low levels of IL-18, caspase-1, ASC and NLRP1/3, decreased STAT3 phosphorylation and high levels of IFN- β and IL-10 transcripts as well as increased phosphorylation of STAT1. An earlier study showed that during *T. gondii* infection in mice, MAPK1 and MAPK2 sensitize the nucleotide-binding domain and leucine-rich repeat-containing protein NLRP1/3 inflammasomes that mediate mouse resistance to infection (Wang et al., 2016). Findings obtained in the present and previous studies support the evidence for the immunostimulatory role of the putative ERK7 protein in regulating *T. gondii* parasite proliferation and in mediating host response to *T. gondii* infection.

In conclusion, we investigated the potential of TgERK7 protein-based immunization for conferring protection in BALB/c mice against *T. gondii* infection. Immunization did not elicit potent humoral immunity as indicated by the lack of increased total IgG and anti-full-length TgERK7 Ab levels following immunization. By contrast, TgERK7-immunization induced significant increase in anti-peptide A Ab titers, suggesting the immunogenicity of this peptide. Congruently, out of the five TgERK7 peptides only anti-peptide A Ab exerted an inhibitory activity against growth of *T. gondii* tachyzoites *in vitro*. Interestingly, immune response induced by immunization with TgERK7 was sufficient to impart protective immunity to *T. gondii* infection as evidenced by the improved survival rate of BALB/c mice infected by virulent GT1 type I strain and the considerable reduction of the parasite cyst burden in the brains of mice infected by type II PRU strain. Further examination of the possible therapeutic efficacy and immune correlates that underpin the anti-parasitic activity of TgERK7 peptide A is warranted.

5. Funding

The work was supported by the Natural Science Funds of Guangxi and Anhui Provinces (2019GXNSFBA185031 & 1908085QC117), the Autonomous Topic of Guangxi Key Laboratory of Brain and Cognitive

Neuroscience (GKLBCN-20180102), the Introduced Doctoral Research Project of Guilin Medical University (31304018021), the Open Fund of the State Key Laboratory of Veterinary Etiological Biology (SKLVEB2016KFKT015), the International Science and Technology Cooperation Project of Gansu Provincial Key Research and Development Program (17JR7WA031), and the Agricultural Science and Technology Innovation Program (ASTIP) (CAAS-ASTIP-2016-LVRI-03).

Declaration of Competing Interest

All the authors declare no conflicts of interest.

Acknowledgments

We would like to thank the University of Nottingham HPC facility for providing large scale resources for parallel computing, the EPSRC for the U1 server grant and the NVIDIA Corporation for the equipment grant used in the GPU-enhanced calculations.

Appendix A. Supplementary data

Supplementary material related to this article can be found, in the online version, at doi:<https://doi.org/10.1016/j.ijmm.2020.151432>.

References

- Abriata, L.A., Dal Peraro, M., 2015. Assessing the potential of atomistic molecular dynamics simulations to probe reversible protein-protein recognition and binding. *Sci. Rep.* 5, 10549. <https://doi.org/10.1038/srep10549>.
- Antunes, D.A., Devaurs, D., Kavasaki, L.E., 2015. Understanding the challenges of protein flexibility in drug design. *Expert Opin. Drug Discov.* 10, 1301–1313. <https://doi.org/10.1517/17460441.2015.1094458>.
- Bengs, F., Scholz, A., Kuhn, D., Wiese, M., 2005. LmxMPK9, a mitogen-activated protein kinase homologue affects flagellar length in *Leishmania mexicana*. *Mol. Microbiol.* 55, 1606–1615. <https://doi.org/10.1111/j.1365-2958.2005.04498.x>.
- Berriz, G.F., King, O.D., Bryant, B., Sander, C., Roth, F.P., 2003. Characterizing gene sets with FuncAssociate. *Bioinformatics* 19, 2502–2504. <https://doi.org/10.1093/bioinformatics/btg363>.
- Berzofsky, J.A., 1985. Intrinsic and extrinsic factors in protein antigenic structure. *Science* 229, 932–940. <https://doi.org/10.1126/science.2410982>.
- Braun, L., Brenier-Pinchart, M.P., Yogavel, M., Curt-Varesano, A., Curt-Bertini, R.L., Hussain, T., Kieffer-Jaquinod, S., Couste, Y., Pelloux, H., Tardieux, I., Sharma, A., Belrhali, H., Bougdour, A., Hakimi, M.A., 2013. A *Toxoplasma dense granule protein*, GRA24, modulates the early immune response to infection by promoting a direct and sustained host p38 MAPK activation. *J. Exp. Med.* 210, 2071–2086. <https://doi.org/10.1084/jem.20130103>.
- Bretou, M., Kumari, A., Malbec, O., Moreau, H.D., Obino, D., Pierobon, P., Randrian, V., Sáez, P.J., Lennon-Duménil, A.M., 2016. Dynamics of the membrane-cytoskeleton interface in MHC class II-restricted antigen presentation. *Immunol. Rev.* 272, 39–51. <https://doi.org/10.1111/imr.12429>.
- Brumlik, M.J., Wei, S., Finstad, K., Nesbit, J., Hyman, L.E., Lacey, M., Burow, M.E., Curiel, T.J., 2004. Identification of a novel mitogen-activated protein kinase in *Toxoplasma gondii*. *Int. J. Parasitol.* 34, 1245–1254. <https://doi.org/10.1016/j.ijpara.2004.07.007>.
- Brumlik, M.J., Pandeswara, S., Ludwig, S.M., Jeansonne, D.P., Lacey, M.R., Murthy, K., Daniel, B.J., Wang, R.F., Thibodeaux, S.R., Church, K.M., Hurez, V., Kious, M.J., Zhang, B., Alagbala, A., Xia, X., Curiel, T.J., 2013. TgMAPK1 is a *Toxoplasma gondii* MAP kinase that hijacks host MKK3 signals to regulate virulence and interferon- γ -mediated nitric oxide production. *Exp. Parasitol.* 134, 389–399. <https://doi.org/10.1016/j.exppara.2013.03.016>.
- Cao, L., Wang, Z., Wang, S., Li, J., Wang, X., Wei, F., Liu, Q., 2016. Deletion of mitogen-activated protein kinase 1 inhibits development and growth of *Toxoplasma gondii*. *Parasitol. Res.* 115, 797–805. <https://doi.org/10.1007/s00436-015-4807-2>.
- Cargnello, M., Roux, P.P., 2011. Activation and function of the MAPKs and their substrates, the MAPK-activated protein kinases. *Microbiol. Mol. Biol. Rev.* 75, 50–83. <https://doi.org/10.1128/MMBR.00031-10>.
- Chatr-Aryamontri, A., Oughtred, R., Boucher, L., Rust, J., Chang, C., Kolas, N.K., O'Donnell, L., Oster, S., Theesfeld, C., Sellam, A., Stark, C., Breitkreutz, B.J., Dolinski, K., Tyers, M., 2017. The BioGRID interaction database: 2017 update. *Nucleic Acids Res.* 45, D369–D379. <https://doi.org/10.1093/nar/gkw1102>.
- Chavarría-Smith, J., Vance, R.E., 2015. The NLRP1 inflammasomes. *Immunol. Rev.* 265, 22–34. <https://doi.org/10.1111/imr.12283>.
- Chen, J., Huang, C., Zhu, D., Shen, P., Duan, Y., Wang, J., Yang, C., Wu, L., 2017. Chinese 1 strain of *Toxoplasma gondii* excreted-secreted antigens negatively modulate Foxp3 via inhibition of the TGF β RII/Smad2/Smad3/Smad4 pathway. *J. Cell. Mol. Med.* 21, 1944–1953. <https://doi.org/10.1111/jcmm.13115>.

- Denkers, E.Y., Gazzinelli, R.T., 1998. Regulation and function of T-cell-mediated immunity during *Toxoplasma gondii* infection. *Clin. Microbiol. Rev.* 11, 569–588. <https://www.ncbi.nlm.nih.gov/pmc/articles/PMC88897/>.
- Dvorakova-Hortova, K., Sidlova, A., Ded, L., Hladovcova, D., Vieweg, M., Weidner, W., Steger, K., Stopka, P., Paradowska-Dogan, A., 2014. *Toxoplasma gondii* decreases the reproductive fitness in mice. *PLoS One* 9, e96770. <https://doi.org/10.1371/journal.pone.0096770>.
- Dyson, H.J., Wright, P.E., 2005. Intrinsically unstructured proteins and their functions. *Nat. Rev. Mol. Cell Biol.* 6, 197–208. <https://doi.org/10.1038/nrm1589>.
- Ellis 4th, J.G., Davila, M., Chakrabarti, R., 2003. Potential involvement of extracellular signal-regulated kinase 1 and 2 in encystation of a primitive eukaryote, *Giardia lamblia*. Stage-specific activation and intracellular localization. *J. Biol. Chem.* 278, 1936–1945. <https://doi.org/10.1074/jbc.M209274200>.
- Elsheikha, H.M., 2008. Congenital toxoplasmosis: priorities for further health promotion action. *Public Health* 122, 335–353. <https://doi.org/10.1016/j.puhe.2007.08.009>.
- Fallahi, S., Rostami, A., Nourollahpour Shiadeh, M., Behniafar, H., Pakinat, S., 2018. An updated literature review on maternal-fetal and reproductive disorders of *Toxoplasma gondii* infection. *J. Gynecol. Obstet. Hum. Reprod.* 47, 133–140. <https://doi.org/10.1016/j.jogoh.2017.12.003>.
- Francia, M.E., Striepen, B., 2014. Cell division in apicomplexan parasites. *Nat. Rev. Microbiol.* 12, 125–136. <https://doi.org/10.1038/nrmicro3184>.
- Gazzinelli, R., Xu, Y., Hieny, S., Cheever, A., Sher, A., 1992. Simultaneous depletion of CD4+ and CD8+ T lymphocytes is required to reactivate chronic infection with *Toxoplasma gondii*. *J. Immunol.* 149, 175–180. <https://www.jimmunol.org/content/149/1/175.long>.
- Gazzinelli, R.T., Wyszocka, M., Hieny, S., Scharon-Kersten, T., Cheever, A., Kühn, R., Müller, W., Trinchieri, G., Sher, A., 1996. In the absence of endogenous IL-10, mice acutely infected with *Toxoplasma gondii* succumb to a lethal immune response dependent on CD4+ T cells and accompanied by overproduction of IL-12, IFN-gamma and TNF-alpha. *J. Immunol.* 157, 798–805. <https://doi.org/10.1029/2011GM001169>.
- Hakimi, M.A., Olias, P., Sibley, L.D., 2017. *Toxoplasma* effectors targeting host signaling and transcription. *Clin. Microbiol. Rev.* 30, 615–645. <https://doi.org/10.1128/CMR.00005-17>.
- Huang, H., Ma, Y.F., Bao, Y., Lee, H., Lisanti, M.P., Tanowitz, H.B., Weiss, L.M., 2011. Molecular cloning and characterization of mitogen-activated protein kinase 2 in *Toxoplasma gondii*. *Cell Cycle* 10, 3519–3526. <https://doi.org/10.4161/cc.10.20.17791>.
- Hunter, C.A., Subauste, C.S., Van Cleave, V.H., Remington, J.S., 1994. Production of gamma interferon by natural killer cells from *Toxoplasma gondii*-infected SCID mice: regulation by interleukin-10, interleukin-12, and tumor necrosis factor alpha. *Infect. Immun.* 62, 2818–2824. <https://iaa.asm.org/content/62/7/2818.long>.
- Huttlin, E.L., Bruckner, R.J., Paulo, J.A., Cannon, J.R., Ting, L., Baltier, K., Colby, G., Gebreab, F., Gygi, M.P., Parzen, H., Szpyt, J., Tam, S., Zarraga, G., Pontano-Vaites, L., Swarup, S., White, A.E., Schweppe, D.K., Rad, R., Erickson, B.K., Obar, R.A., Guruharsha, K.G., Li, K., Artavanis-Tsakonas, S., Gygi, S.P., Harper, J.W., 2017. Architecture of the human interactome defines protein communities and disease networks. *Nature* 545, 505–509. <https://doi.org/10.1038/nature22366>.
- Ibrahim, H.M., Xuan, X., Nishikawa, Y., 2010. *Toxoplasma gondii* cyclophilin 18 regulates the proliferation and migration of murine macrophages and spleen cells. *Clin. Vaccine Immunol.* 17, 1322–1329. <https://doi.org/10.1128/CVI.00128-10>.
- Jo, S., Kim, T., Iyer, V.G., Im, W., 2008. CHARMM-GUI: a web-based graphical user interface for CHARMM. *J. Comput. Chem.* 29, 1859–1865. <https://doi.org/10.1002/jcc.20945>.
- Kamiyama, T., Hagiwara, T., 1982. Augmented followed by suppressed levels of natural cell-mediated cytotoxicity in mice infected with *Toxoplasma gondii*. *Infect. Immun.* 36, 628–636. <https://iaa.asm.org/content/36/2/628.long>.
- Kanatani, S., Fuks, J.M., Olafsson, E.B., Westermarck, L., Chambers, B., Varas-Godoy, M., Uhlen, P., Barragan, A., 2017. Voltage-dependent calcium channel signaling mediates GABAA receptor-induced migratory activation of dendritic cells infected by *Toxoplasma gondii*. *PLoS Pathog.* 13, e1006739. <https://doi.org/10.1371/journal.ppat.1006739>.
- Kelley, L.A., Mezulis, S., Yates, C.M., Wass, M.N., Sternberg, M.J., 2015. The Phyre2 Web Portal for Protein Modeling, Prediction and. <https://doi.org/10.1038/nprot.2015.053>.
- Kim, K., Weiss, L.M., 2008. *Toxoplasma*: the next 100 years. *Microbes Infect.* 10, 978–984. <https://doi.org/10.1016/j.micinf.2008.07.015>.
- Kortagere, S., 2012. Screening for small molecule inhibitors of *Toxoplasma gondii*. *Expert Opin. Drug Discov.* 7, 1193–1206. <https://doi.org/10.1517/17460441.2012.729036>.
- Kyosseva, S.V., 2004. Mitogen-activated protein kinase signaling. *Int. Rev. Neurobiol.* 59, 201–220. [https://doi.org/10.1016/S0074-7742\(04\)59008-6](https://doi.org/10.1016/S0074-7742(04)59008-6).
- Li, Z.Y., Chen, J., Petersen, E., Zhou, D.H., Huang, S.Y., Song, H.Q., Zhu, X.Q., 2014. Synergy of mIL-21 and mIL-15 in enhancing DNA vaccine efficacy against acute and chronic *Toxoplasma gondii* infection in mice. *Vaccine* 32, 3058–3065. <https://doi.org/10.1016/j.vaccine.2014.03.042>.
- Li, Z.Y., Wang, Z.D., Huang, S.Y., Zhu, X.Q., Liu, Q., 2016. TgERK7 is involved in the intracellular proliferation of *Toxoplasma gondii*. *Parasitol. Res.* 115, 3419–3424. <https://doi.org/10.1007/s00436-016-5103-5>.
- Li, Z.Y., Guo, H.T., Tan, J., Geng, Z.Y., Zhu, X.Q., 2020. Devaluation of the immune mapped protein 1 undermines the intracellular proliferation of *Toxoplasma gondii*. *Exp. Parasitol.* 211, 107843. <https://doi.org/10.1016/j.exppara.2020.107843>.
- Lüder, C.G.K., Rahman, T., 2017. Impact of the host on *Toxoplasma* stage differentiation. *Microb. Cell* 4, 203–211. <https://doi.org/10.15698/mic2017.07.579>.
- Lye, Y.M., Chan, M., Sim, T.S., 2006. Pfnek3: an atypical activator of a MAP kinase in *Plasmodium falciparum*. *FEBS Lett.* 580, 6083–6092. <https://doi.org/10.1016/j.febslet.2006.10.003>.
- Nabi, H., Rashid, I., Ahmad, N., Durrani, A., Akbar, H., Islam, S., Bajwa, A.A., Shehbaz, M., Ashraf, K., Imran, N., 2017. Induction of specific humoral immune response in mice immunized with ROP18 nanospheres from *Toxoplasma gondii*. *Parasitol. Res.* 116, 359–370. <https://doi.org/10.1007/s00436-016-5298-5>.
- Ochiai, E., Sa, Q., Perkins, S., Grigg, M.E., Suzuki, Y., 2016. CD8(+) T cells remove cysts of *Toxoplasma gondii* from the brain mostly by recognizing epitopes commonly expressed by or cross-reactive between type II and type III strains of the parasite. *Microbes Infect.* 18, 517–522. <https://doi.org/10.1016/j.micinf.2016.03.013>.
- Omata, Y., Kawano, T., Ohsawa, T., Sugaya, S., Satake, M., Isamida, T., Koyama, T., Taka, A., Miyazawa, K., Takagi, M., Saito, A., Toyoda, Y., 1999. Infectivity of feline enteropathogenic stages of *Toxoplasma gondii* isolated by Percoll-density gradient centrifugation. *Vet. Parasitol.* 82, 211–215. [https://doi.org/10.1016/s0304-4017\(99\)00019-9](https://doi.org/10.1016/s0304-4017(99)00019-9).
- Orchard, S., Ammari, M., Aranda, B., Breuza, L., Briganti, L., Broackes-Carter, F., Campbell, N.H., Chavali, G., Chen, C., del-Toro, N., Duesbury, M., Dumousseau, M., Galeota, E., Hinz, U., Iannuccelli, M., Jagannathan, S., Jimenez, R., Khadake, J., Lagreid, A., Licata, L., Lovering, R.C., Meldal, B., Melidoni, A.N., Milagros, M., Peluso, D., Perfetto, L., Porras, P., Raghunath, A., Ricard-Blum, S., Roehert, B., Stutz, A., Tognoli, M., van Roey, K., Cesareni, G., Hermjakob, H., 2014. The MintAct project—IntAct as a common curation platform for 11 molecular interaction databases. *Nucleic Acids Res.* 42, D358–D363. <https://doi.org/10.1093/nar/gkt1115>.
- Petersen, E.F., Goddard, T.D., Huang, C.C., Couch, G.S., Greenblatt, D.M., Meng, E.C., Ferrin, T.E., 2004. UCSF Chimera—a visualization system for exploratory research and analysis. *J. Comput. Chem.* 25, 1605–1612. <https://doi.org/10.1002/jcc.20084>.
- Phillips, J.C., Braun, R., Wang, W., Gumbart, J., Tajkhorshid, E., Villa, E., Chipot, C., Skeel, R.D., Kalé, L., Schulten, K., 2005. Scalable molecular dynamics with NAMD. *J. Comput. Chem.* 26, 1781–1802. <https://doi.org/10.1002/jcc.20289>.
- Portillo, J.C., Muniz-Feliciano, L., Lopez Corcino, Y., Lee, S.J., Van Grol, J., Parsons, S.J., Schiemann, W.P., Subauste, C.S., 2017. *Toxoplasma gondii* induces FAK-Src-STAT3 signaling during infection of host cells that prevents parasite targeting by autophagy. *PLoS Pathog.* 13, e1006671. <https://doi.org/10.1371/journal.ppat.1006671>.
- Rougier, S., Montoya, J.G., Peyron, F., 2017. Lifelong persistence of *Toxoplasma* cysts: a questionable dogma? *Trends Parasitol.* 33, 93–101. <https://doi.org/10.1016/j.pt.2016.10.007>.
- Rytel, M.W., Jones, T.C., 1966. Induction of interferon in mice infected with *Toxoplasma gondii*. *Proc. Soc. Exp. Biol. Med.* 123, 859–862. <https://doi.org/10.3181/00379727-123-31624>.
- Sasai, M., Pradipa, A., Yamamoto, M., 2018. Host immune responses to *Toxoplasma gondii*. *Int. Immunol.* 30, 113–119. <https://doi.org/10.1093/intimm/dxy004>.
- Schlüter, D., Däubener, W., Schares, G., Groß, U., Pleyer, U., Lüder, C., 2014. Animals are key to human toxoplasmosis. *Int. J. Med. Microbiol.* 304, 917–929. <https://doi.org/10.1016/j.ijmm.2014.09.002>.
- Shannon, P., Markiel, A., Ozier, O., Baliga, N.S., Wang, J.T., Ramage, D., Amin, N., Schwikowski, B., Ideker, T., 2003. Cytoscape: a software environment for integrated models of biomolecular interaction networks. *Genome Res.* 13, 2498–2504. <https://doi.org/10.1101/gr.1239303>.
- Sloan, T.J., Murray, E., Yokoyama, M., Massey, R.C., Chan, W.C., Bonev, B.B., Williams, P., 2019. Timing is everything: impact of naturally occurring *Staphylococcus aureus* AgrC cytoplasmic domain adaptive mutations on autoinduction. *J. Bacteriol.* 201 (20), e00409–e00419. <https://doi.org/10.1128/JB.00409-19>. pii.
- Sommerville, C., Richardson, J.M., Williams, R.A., Mottram, J.C., Roberts, C.W., Alexander, J., Henriquez, F.L., 2013. Biochemical and immunological characterization of *Toxoplasma gondii* macrophage migration inhibitory factor. *J. Biol. Chem.* 288, 12733–12741. <https://doi.org/10.1074/jbc.M112.419911>.
- Suzuki, Y., Remington, J.S., 1988. Dual regulation of resistance against *Toxoplasma gondii* infection by Lyt-2+ and Lyt-1+ L3T4+ T cells in mice. *J. Immunol.* 140, 3943–3946. <https://www.jimmunol.org/content/140/11/3943.long>.
- Suzuki, Y., Wang, X., Jortner, B.S., Payne, L., Ni, Y., Michie, S.A., Xu, B., Kudo, T., Perkins, S., 2010. Removal of *Toxoplasma gondii* cysts from the brain by perforin-mediated activity of CD8+ T cells. *Am. J. Pathol.* 176, 1607–1613. <https://doi.org/10.2353/ajpath.2010.090825>.
- Szabo, E.K., Finney, C.A.M., 2017. *Toxoplasma gondii*: one organism, multiple models. *Trends Parasitol.* 33, 113–127. <https://doi.org/10.1016/j.pt.2016.11.007>.
- Szklarczyk, D., Morris, J.H., Cook, H., Kuhn, M., Wyder, S., Simonovic, M., Santos, A., Doncheva, N.T., Roth, A., Bork, P., Jensen, L.J., von Mering, C., 2017. The STRING database in 2017: quality-controlled protein-protein association networks, made broadly accessible. *Nucleic Acids Res.* 45, D362–D368. <https://doi.org/10.1093/nar/gkw937>.
- Thouvenin, M., Candolfi, E., Villard, O., Klein, J.P., Kien, T., 1997. Immune response in a murine model of congenital toxoplasmosis: increased susceptibility of pregnant mice and transplacental passage of *Toxoplasma gondii* are type 2-dependent. *Parasitologia* 39, 279–283. [https://doi.org/10.1016/0022-3697\(62\)90103-8](https://doi.org/10.1016/0022-3697(62)90103-8).
- Wang, S., Wang, Z., Gu, Y., Li, Z., Li, Z., Wei, F., Liu, Q., 2016. *Toxoplasma gondii* mitogen-activated protein kinases are associated with inflammatory activation in infected mice. *Microbes Infect.* 18, 696–700. <https://doi.org/10.1016/j.micinf.2016.07.004>.
- Zhang, Y., 2008. I-TASSER server for protein 3D structure prediction. *BMC Bioinformatics* 9, 40. <https://doi.org/10.1186/1471-2105-9-40>.
- Zhang, F., Strand, A., Robbins, D., Cobb, M.H., Goldsmith, E.J., 1994. Atomic structure of the MAP kinase ERK2 at 2.3 Å resolution. *Nature* 367, 704–711. <https://doi.org/10.1038/367704a0>.